Analysis and Design of a W-Band MMIC LNA with 4.2 dB Noise Figure in GaAs-based 100 nm pHEMT Technology

Galip Orkun ARICAN[1*] (ID)   Burak Alptuğ YILMAZ[2] (ID)

[1] ASELSAN Inc, Communication and Information Technologies Division, Ankara, Türkiye

Keywords	Abstract
THz W-band MMIC GaAs pHEMT mm-Wave	A W-band Monolithic Microwave Integrated Circuit (MMIC) Low Noise Amplifier (LNA) is presented in this paper. The UMS PH10 process, which is the GaAs/InGaAs based pseudomorphic High Electron Mobility Transistors (pHEMTs) technology, is utilized to design the proposed W-band MMIC LNA. The proposed LNA has a simulated noise figure (NF) of 4.2 dB in the operating frequency range from 94 to 104 GHz while the simulated minimum noise figure (NF_{min}) of 3.9 dB at the center frequency. Besides, proposed W-band MMIC LNA has very good reflection loss performance, well below -10 dB and high small signal gain (S_{21}), above 16.3 dB. Moreover, MMIC LNA is unconditionally stable up to 160 GHz. Furthermore, the proposed 3-stage MMIC LNA has a total DC power dissipation of 120 mW DC while drain voltage is 2 V. The proposed W-band LNA has a small size of 2.2 mm x 1.2 mm which yields a total chip size of 2.64 mm^2.

1. INTRODUCTION

The improvements in technology increase functionality and flexibility of communication platforms by increasing operating frequency band and reducing system dimensions (Arican et al., 2019). Radar architecture, especially spaceborne cloud profiling radars and automotive radars, fifth generation (5G) base stations and high frequency active electronically scanning arrays (AESAs) have benefited from these technological advances (Arıcan & Yılmaz, 2024). Therefore, the necessity of millimeter-Wave (mm-Wave) radio frequency (RF) components has been increased to deploy in modern communication systems (Murthy et al., 2024). In the meantime, upward trend in the use of modern communication systems has emerged a great demand for high-data-rate and ultra-wide bandwidth communication. So as to meet this necessity, W-band (75 GHz – 110 GHz) has a huge potential for new generation communication systems with its low-latency, high data rate and wide bandwidth advantageous (Tong et al., 2020). Hence, the benefits and drawbacks of W-band communication systems have been investigated in literature for many years (Leuther et al., 2009; Liu et al., 2019; Longhi et al., 2025; Thome at al., 2020; Thome et al., 2022; Wang et al., 2024). Besides, internet of things (IoT) technology has become popular, gradually. It gives a chance to enhance human beings' lives because any of objects can communicate with each other with high speed data rates. Low atmospheric loss,

wide operating frequency bandwidth and short wavelength advantageous of W-band frequencies provide to design versatile and long-range communication systems especially in space/satellite platforms as a main carrier. Moreover, the most general digital modulation techniques such as binary phase shift keying (BPSK) are well suited in W-band satellite systems which have high data rate capability. Furthermore, while the number of devices that are linked to one network like one base station has been rising, the demand for high data rates and wide bandwidth has been essential. Finally, W-band with profits of high temperature sensitivity and advanced resolution is very critical for medical imaging systems and sensors (Cuadrado-Calle et al., 2024; Gao et al., 2020).

In addition, the frequency allocation system of W-band with fixed 5 GHz bandwidth results in designing simple and compact transmitter and receiver devices in comparison with Q-band and V-band which are commonly utilized for communication systems from past to present. Therefore, the necessity of W-band RF components such as LNAs, power amplifiers (PAs), couplers, power dividers/combiners and circulators, has gone up. These RF components must be compatible with space and airborne platforms, if their operating frequencies are in W-band spectrum. So as to develop W-band systems, there are a couple of MMIC process technologies such as GaAs, Indium Phosphate (InP), Silicon Germanium (SiGe), Silicon on Insulator (SOI) and Gallium Nitride (GaN) which are the most known substrate materials to fabricate MMICs. Although GaN based MMICs come to the forefront in case of their high-power density and compact design advantageous, GaAs based devices have given chance to achieve cost effective solutions (Kobayashi & Kumar, 2021).

In this paper, a W-band MMIC LNA is presented with simulation results and design constraints. The paper is organized as an introduction, MMIC process and LNA design, simulation results and discussion and conclusion parts, respectively. During the design, proper HEMT has been chosen from PH10 GaAs pHEMT process design kit (PDK) of United Monolithic Semiconductors (UMS) company according to small and large signal measurements and DC-IV characterizations of pHEMTs included in its library. HEMTs in the library have been fabricated in 0.1 μm very low-noise high gain GaAs pHEMT based technology considering RF performances. The proposed MMIC LNA operates with small signal gain (S_{21}) of 16.3 dB and noise figure (NF) of 4.2 dB. However, it is important that NF_{min} is 3.9 dB at 99 GHz which is the center of the operating frequency. Moreover, the LNA operates in the frequency range from 94 GHz to 104 GHz with 10 GHz bandwidth which yields a fractional bandwidth of approximately 10%. The device operates with very good input and output (I/O) reflection losses performance which are lower than -10 dB. Thus, it is convenient to deploy any system that required maximum 10% power reflection. Additionally, the proposed design is unconditionally stable up to 160 GHz. Thus, it can be said that there are not any oscillation mechanisms, and the stability factor is always higher than 1 up to 160 GHz. Additionally, it consumes 120 mW DC power while drain to source voltage (V_{ds}) is 2 V. Finally, the proposed device has very competitive dimensions of 2.2 x 1.2 mm^2.

2. MMIC PROCESS AND LNA DESIGN

In the W-band MMIC LNA design, the PH10 process, which is provided by United Monolithic Semiconductors (UMS), was utilized. The PH10 is a GaAs/InGaAs pseudomorphic high electron mobility transistor (pHEMT) technology with a short 100 nm gate length which optimized by UMS to have high linear gain and low noise performance up to 110 GHz. In addition, the PH10 process has consisted of two interconnect metallization layers, metal-insulator-metal (MIM) capacitors, Tantalum Nitride (TaN) resistor, Titanium Tungsten Silisium (TiWSi) resistors, airbridges and via holes. Besides, the schematic and layout design of the proposed W-band LNA was performed with utilizing Keysight's commercially available Advanced Design System (ADS) software and the UMS PH10 PDK was introduced to ADS. In the electromagnetic (EM) simulations ADS software's Momentum tool was utilized to solve the EM numerical analysis with utilizing Method of Moments.

In the first step of the design, a numerous Direct Current (DC) and Radio Frequency (RF) simulations were performed for different size of gate peripheries. In the simulations, a variety of different gate periphery was tried to achieve the minimum noise figure (NF_{min}) and optimum gain performance. So as to achieve this, the gate periphery of 4x50 μm was chosen because of its 280 mA/mm current density and 725 mS/mm transconductance. In addition, the gate and drain voltages were swept to check the both noise and maximum available gain (*MAG*) performance of the 4x50 μm pHEMT. According to the simulation results, it was observed that NF_{min} of the 4x50 μm pHEMT was at around 3.6 dB when the gate to source voltage (V_{gs}) was -0.3 V and the drain to source voltage (V_{ds}) was 2V for 100 GHz at ambient temperature as seen in the Figure 1. Moreover, it was also observed that the MAG is greater than 6.3 dB for 100 GHz at ambient temperature when the V_{gs} and V_{ds} were respectively -0.3 V and 2 V as seen in the Figure 2.

In the LNA design process, the noise factor (*F*) and *NF* are the crucial figure of merits (FoM) of the distortion in the signal to noise ratio (SNR), which is the ratio of signal power density to noise power density caused by the signal chain of the network (Arican et al., 2019; Arican et al., 2021; Arican & Akcam, 2023). As given in the Equation 1, *F* and *NF* are related to each other, while the *F* is a unitless FoM, *NF* can be demonstrated as the logarithm of *F* in unit of decibels [dB].

$$NF = 10 \, \log_{10} F \; [dB] \tag{1}$$

The *F* is expressed as the ratio of the output noise power of a device to the portion of the thermal noise at the input port attributable at the standard noise temperature of 290 K. In other words, the *F* also can be described as the ratio of the input to output SNR as given in the Equation 2.

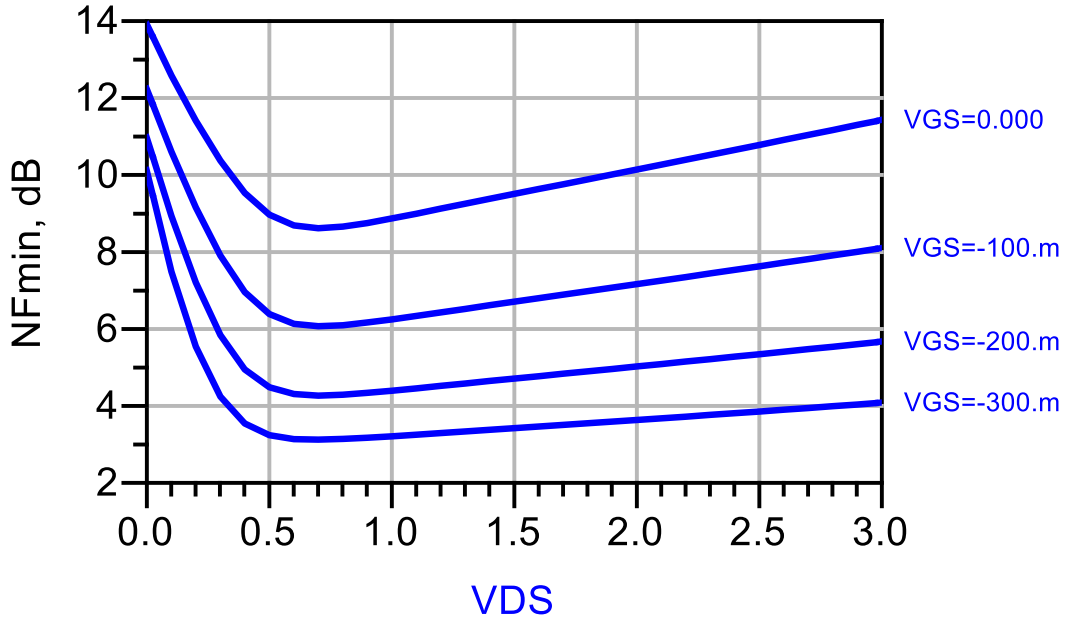$$F = \frac{SNR_i}{SNR_o} \tag{2}$$

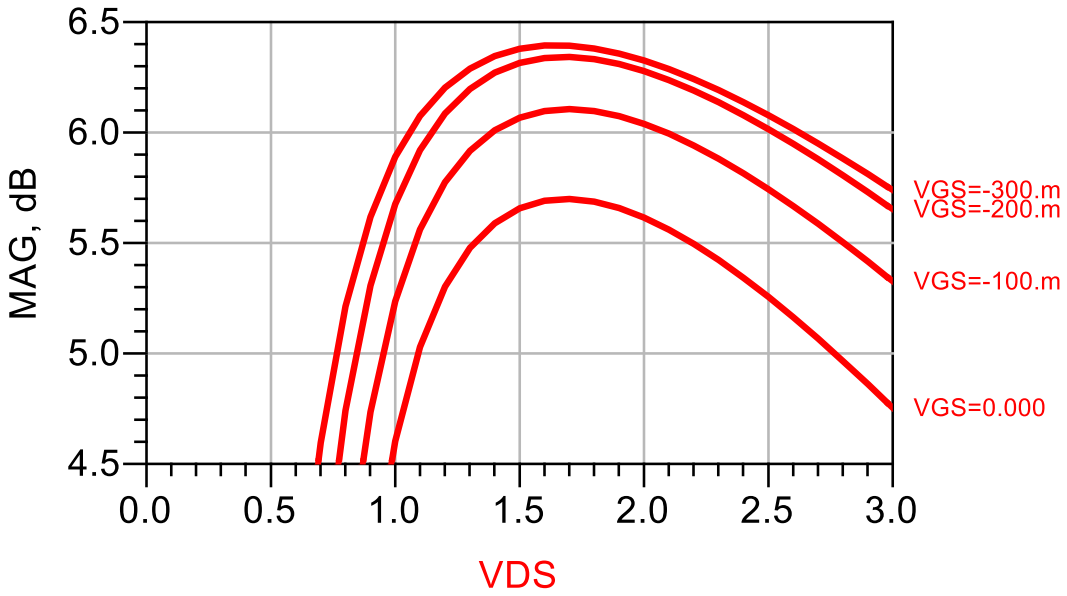**Figure 1.** *Simulation Results of NF_{min} at 100 GHz for 4x50 µm pHEMT*

Figure 2. *Simulation Results of MAG at 100 GHz for 4x50 µm pHEMT*

In addition, the *F* can be expressed as a function of reflection coefficient as given in the Equation 3.

$$F = F_{min} + \frac{R_n}{G_s}\left|Y_s - Y_{opt}\right|^2 \qquad (3)$$

where Y_s and Y_{opt} indicates the source admittance ($Y_s = G_s + jB_s$ & $Y_s = 1/Z_s$) and optimum input admittance ($Y_{opt} = G_{opt} + jB_{opt}$), Z_0 is the characteristic impedance, R_n indicates the equivalent noise resistance and G_s indicates the real part of Y_s.

On the other hand, the Lange invariant parameter of *N*, which is the sensitivity of the noise factor between Y_s and Y_{opt}, is related to R_n via $N = R_n \cdot G_{opt}$. The *F* can be expressed as given in the Equation 4.

$$F = F_{min} + \frac{N}{G_{opt} G_s} |Y_s - Y_{opt}|^2 \tag{4}$$

By utilizing $F_{min}-1 \approx 2N$, the Equation 3 can be simplified as given Equation 5.

$$F \approx F_{min} + \frac{NF_{min} - 1}{2 G_{opt} G_s} |Y_s - Y_{opt}|^2 \tag{5}$$

After choosing proper pHEMT, input and output impedance values with respect to gain and power targets, stability factor and noise figure specifications of MMIC LNA were defined. It is aimed that the device has worked between 94 GHz to 104 GHz with the gain of higher than 16 dB and better than 5 dB *NF* performances. In the design specifications, the minimum noise performance can be achieved with matching the source impedance (Z_s) to the optimum input impedance (Z_{opt}) as observed in the Equation 5. In the light of this fact, the load-pull and source-pull simulations was performed to define input and output impedance values of 4x50 μm pHEMTs with respect to gain and power targets, stability factor and noise figure specifications of MMIC LNA. In addition, the Z_s was matched the Z_{opt} (12.3-j*7.4) for the 4x50 μm pHEMTs (Q_1, Q_2 & Q_3). Besides, minimum number of RF components have been deployed in I/O matching networks to decrease their additive effects on *NF*. Moreover, I/O matching networks of each transistor have been matched to 50 Ω impedance to avoid the need for an additional external matching circuit in the module design. On the other hand, in the design, 3-stages LNA has built with connecting 3 identical pHEMT in serial way for meeting S_{21} requirement. Additionally, the gate bias (TL_3, TL_{15} & TL_{24}) and drain bias (TL_7, TL_{12} & TL_{21}) feedlines have been consisted of the transmission line of λ/4 length to protect the DC power supply from undesirable RF signal. Furthermore, radial stub ($Stub_1$, $Stub_2$, $Stub_3$, $Stub_4$, $Stub_5$, $Stub_6$) and shunt MIM capacitors (C_2, C_3, C_5, C_6, C_7, C_8, C_{10}, C_{11}, C_{13}, C_{14}, C_{16} & C_{17}) have been positioned in both input and output terminals to block oscillation mechanisms while and series resistors (R_1, R_2, R_5, R_6, R_8 & R_9) have been placed to increase the stability of the circuit. By the same token, a shunt RC network (R_3C_4, R_4C_9 & R_7C_{15}) have put in input terminals of each stage of LNA as a stabilization circuit. In the stabilization network, a resistor and MIM capacitor have been serially connected to each other and in this way, the gate current cannot flow through the ground while the circuit become stable. Hence, the device works up to 160 GHz with constant current density and without any oscillation. Additionally, serial connected capacitors (C_1, C_{12}, C_{18} & C_{19}) have been utilized between each stage to prevent the DC flow through the RF terminals. The schematic view of MMIC LNA can be seen in Figure 3.

During the design of LNA, a couple of optimizations were performed considering initial circuit schematic. After modeling of RF components such as capacitors, inductors, and resistors, real-like behaviors of these components have been used in electromagnetic (EM) simulations of the proposed device and layout design rules. Besides, the proposed device's 2.5D layout simulations have been performed via Method of Moments (MoM) technique. Additionally, The DC bias pad has a dimension of 100 x 100 μm to be able to have at least 2 pieces of gold (Au) wire bond connections. Furthermore, gate and drain bias points have placed to north and south of the device, respectively for easy of packing and on-wafer measuring. The dimension of the device is

2.2 x 1.2 mm^2 (0.73 λ_0 x 0.4 λ_0 at 100 GHz). The layout of the proposed W-band MMIC LNA can be seen in Figure 4.
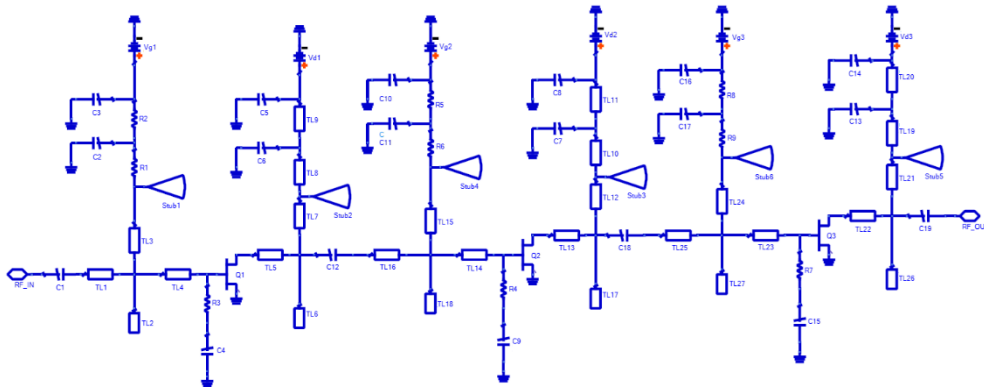

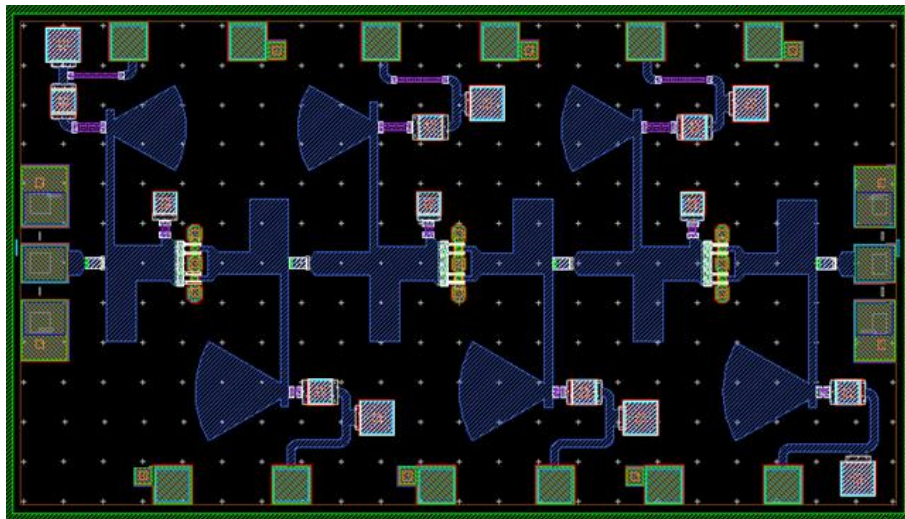*Figure 3. The Proposed MMIC LNA Schematic View*

Figure 4. The layout of the proposed W-band MMIC LNA

3. SIMULATION RESULTS AND DISCUSSION

The summary of electrical and RF performances of the proposed MMIC LNA can be found in Table 1. Performances of I/O matching (S_{11} & S_{22}), gain (S_{21}), stability and *NF* of MMIC LNA are shown in Figure 5, 6, 7 and 8, respectively. According to simulation results, S_{11} and S_{22} are lower than -10 dB while S_{21} is higher than 16.3 dB in the range of operating frequency of 94 GHz – 104 GHz. Moreover, the gain flatness is approximately 0.13 dB/GHz. Secondly, stability performance of the device is higher than 1 up to 160 GHz with delta (Δ), lower than 1. It is crystal clear that proposed LNA is unconditionally stable. Finally, *NF* of the proposed W-band LNA is lower than 4.2 dB over the range of 94 GHz – 104 GHz and *NF$_{min}$* is 3.9 dB at the center frequency of 99 GHz.

The state of the art W-band MMIC LNAs is presented in Table 2. The proposed MMIC LNA has better noise and gain performances compared to study that is fabricated 3-stage with GaAs technology (Tong et al., 2020). It is stated that when 50 nm GaAs technology is preferred, *NF* performance gets better, and bandwidth

increases (Thome et al., 2017). Moreover, if the technology is chosen as above 100 nm, the operating frequency decreases (Tanahashi et al., 2003). According to other studies that are presented in Table 2, if the number of HEMTs used increases, gain performance increases but the proposed device has been already preferable in case of *NF* performance (Li et al., 2020; Sharma et al., 2024; Yawei & Wihua, 2013; Zang et al., 2018). Finally, the proposed MMIC LNA is also very competitive compared to literature in terms of its area of 2.2 x 1.2 mm^2 and power consumption of 120 mW as can be seen in Table 2.

Table 1. *Summary of Electrical and RF Performances*

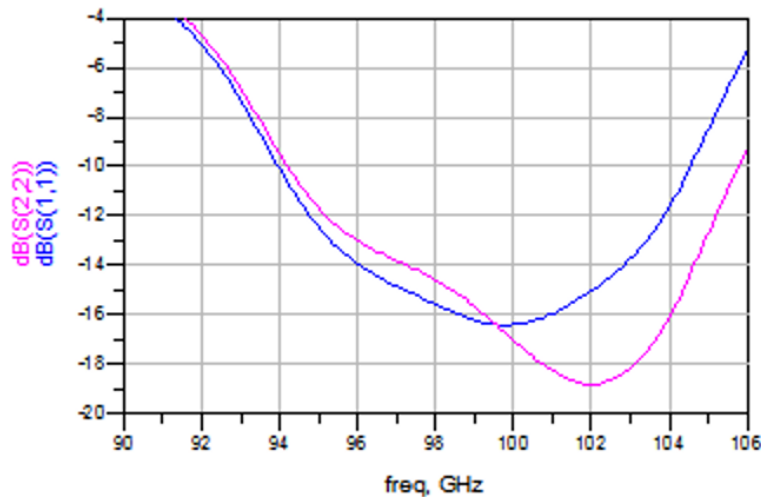|	Value	Unit
Frequency range	94 – 104	GHz
I/O matching	< -10	dB
Gain	> 16.3	dB
Gain Flatness	< 0.13	dB/GHz
NF	< 4.2	dB
Drain voltage	2	V
DC current	60	mA
Stability	Unconditional Stable	-

Figure 5. *Simulation Results of S$_{11}$ and S$_{22}$*

4. CONCLUSION

A W-band MMIC LNA is brought forward in this paper. The presented device is designed with using PH10 PDK of UMS Company and the PDK provides in GaAs Technology HEMTs. According to simulation results, the simulated *NF* of the proposed LNA is across the 3.9-4.2 dB in the operating frequency bandwidth. Additionally, the device operates from 94 GHz to 104 GHz with reflection loss performance better than -10 dB and small signal gain performance better than 16 dB. Furthermore, the LNA works unconditionally stable, and the stability factor is always higher than 1 for whole operating frequency band and up to 160 GHz. Moreover, its P$_{dc}$ is equal to 120 mW and layout dimensions are 2.2 x 1.2 mm^2. As a result, with its prominent features, it is perfect nominee for applications such as high frequency AESAs, 5G communication systems,

IOT applications, medical imaging and sensors that require high data rates, wide bandwidth, high temperature sensitivity and resolution.
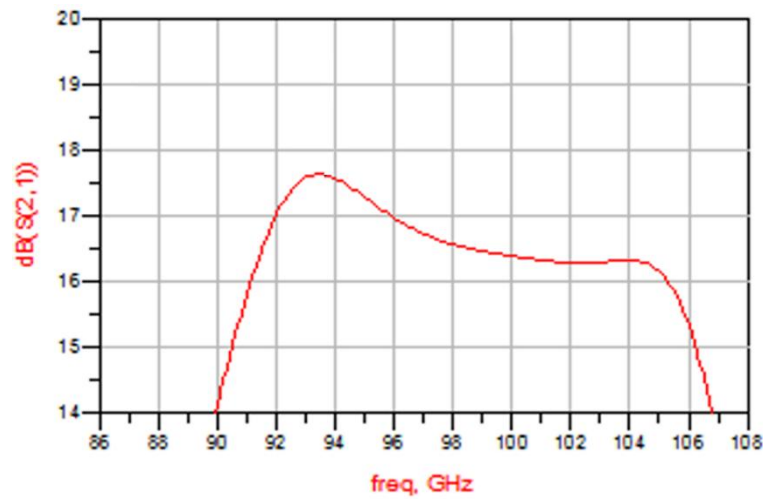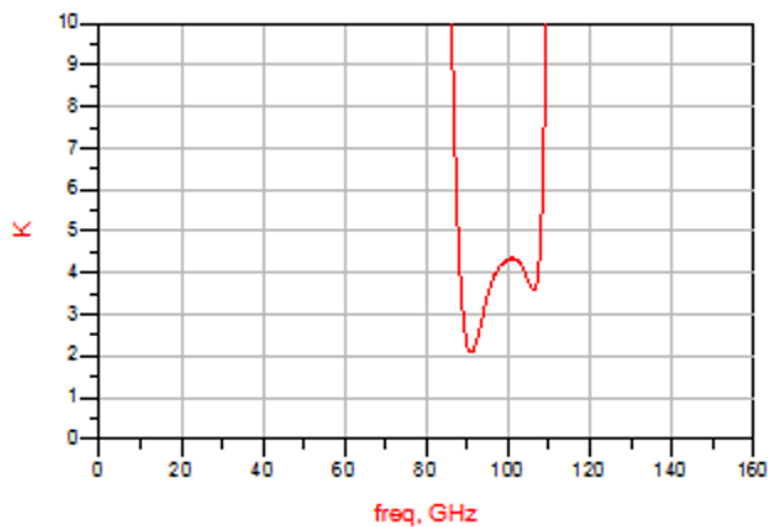

Figure 6. *Simulation Result of S_{21}*

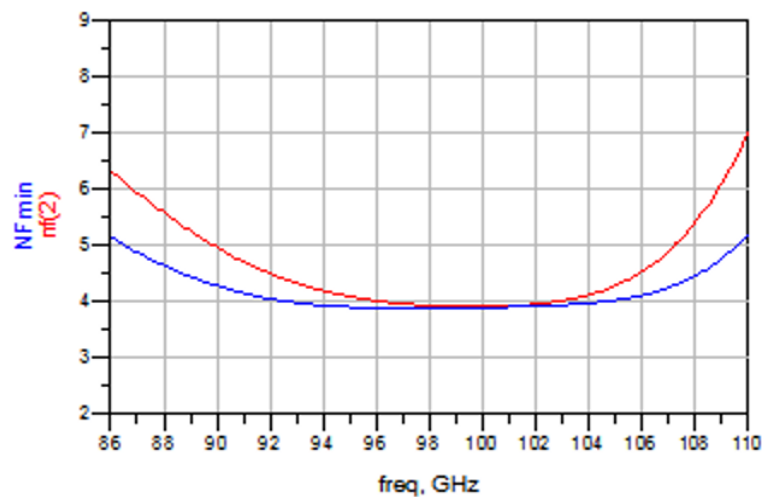***Figure 7.*** *Simulation Result of Stability Factor*

Figure 8. *Simulation Result of NF*

Table 2. State of the Art W-Band MMIC LNAs

Ref	Freq (GHz)	Gain (dB)	NF (dB)	Techn.	Area (mm^2)	# of Stage	Pdc (mW)
Tong et al., 2020	78.5 – 90	14.5	5.2	GaAs (100 nm)	3 x 1.4	3	190
Thome et al., 2017	75 – 110	20	2.6	GaAs (50 nm)	1.5 x 1.0	4	40.8
Tanahashi et al., 2003	76 – 77	15	3.5	GaAs (190 nm)	1.88 x 1.2	3	N/A
Zhang et al., 2018	75 – 110	20	5	GaAs (100 nm)	1.2 x 1.0	4	92
Li et al., 2020	80 – 100	22	5	GaAs (100 nm)	1.48 x 0.66	4	96
Yawei & Weihua, 2013	90 – 113	19	3.2	GaAs (N/A)	1.3 x 0.51	4	N/A
Sharma et al., 2024	92 – 115	19	4.6	GaAs (100 nm)	4.0 x 2.5	4	80
This Work	94 – 104	16.3	4.2	GaAs (100 nm)	2.2 x 1.2	3	120

AUTHOR CONTRIBUTIONS

All authors have read and legally accepted the final version of the article published in the journal.

CONFLICT OF INTEREST

The authors declare no conflict of interest.

REFERENCES

Arıcan, G. O., & Yılmaz, B. A. (2024). A 10-W GaN on SiC CPW MMIC High-Power Amplifier With 44.53% PAE for X-Band AESA Radar Applications. *Electrica*, *24*(3), 780-788. https://doi.org/10.5152/electrica.2024.24090

Arican, G. O., Akcam, N., & Yazgan, E. (2019, April). Ku-band MMIC LNA design for space applications. In *2019 6th International Conference on Electrical and Electronics Engineering (ICEEE)* (pp. 274-278). IEEE. https://doi.org/10.1109/ICEEE2019.2019.00059

Arican, G. O., Dokmetas, B., Akcam, N., & Yazgan, E. (2019, November). 28-36 GHz MMIC LNA Design for Satellite Applications. In *2019 11th International Conference on Electrical and Electronics Engineering (ELECO)* (pp. 726-729). IEEE. https://doi.org/10.23919/ELECO47770.2019.8990444

Arican, G. O., Akcam, N., & Yazgan, E. (2021). Ku-band GaAs mHEMT MMIC and RF front-end module for space applications. *Microwave and Optical Technology Letters*, *63*(2), 417-425. https://doi.org/10.1002/mop.32613

Arican, G. O., & Akcam, N. (2022). Design of a Low Cost X-Band LNA with Sub-1-dB NF for SATCOM Applications. *Gazi University Journal of Science*, 36(1), 208-2018. https://doi.org/10.35378/gujs.998008

Cuadrado-Calle, D., Kantanen, M., Valenta, V., & Ayllón, N. (2024). A GaN-on-Si MMIC LNA for Spaceborne Cloud Profiling Radars and W-Band Telecom Links. *IEEE Microwave and Wireless Technology Letters*, *34*(12), 1359-1362. https://doi.org/10.1109/LMWT.2024.3469276

Gao, L., Wagner, E., & Rebeiz, G. M. (2019). Design of E-and W-band low-noise amplifiers in 22-nm CMOS FD-SOI. *IEEE Transactions on Microwave Theory and Techniques*, *68*(1), 132-143. https://doi.org/10.1109/TMTT.2019.2944820

Kobayashi, K. W., & Kumar, V. (2021). A broadband 70–110-GHz E-/W-band LNA using a 90-nm T-gate GaN HEMT technology. *IEEE Microwave and Wireless Components Letters*, *31*(7), 885-888. https://doi.org/10.1109/LMWC.2021.3076360

Leuther, A., Tessmann, A., Kallfass, I., Losch, R., Seelmann-Eggebert, M., Wadefalk, N., ... & Ambacher, O. (2009, May). Metamorphic HEMT technology for low-noise applications. In *2009 IEEE International Conference on Indium Phosphide & Related Materials* (pp. 188-191). IEEE. https://doi.org/10.1109/ICIPRM.2009.5012475

Li, Z., Yan, P., Chen, J., & Hou, D. (2020, September). A wide-bandwidth W-band LNA in GaAs 0.1 μm pHEMT technology. In *2020 IEEE MTT-S International Wireless Symposium (IWS)* (pp. 1-3). IEEE. https://doi.org/10.1109/IWS49314.2020.9360082

Liu, C., Ren, Q., & Yang, F. (2019, March). A W-band LNA for Passive millimeter wave imaging Application. In *2019 China Semiconductor Technology International Conference (CSTIC)* (pp. 1-3). IEEE. https://doi.org/10.1109/CSTIC.2019.8755738

Longhi, P. E., Colangeli, S., Ciccognani, W., Parand, P., Serino, A., & Limiti, E. (2024). 4.1-dB Noise Figure and 20-dB Gain 92–115-GHz GaAs LNA With Hot Via Interconnections. *IEEE Microwave and Wireless Technology Letters*. https://doi.org/10.1109/LMWT.2024.3520229

Murthy, B. V., Manjushree, T. M., Meghana, N., Ramya, H. G., & Vaishnavi, V. (2024, May). A millimeter Wave MMIC Power Amplifier using 0.15 um GaN for Space Communication Systems. In *2024 International Conference on Smart Systems for applications in Electrical Sciences (ICSSES)* (pp. 1-6). IEEE. https://doi.org/10.1109/ICSSES62373.2024.10561334

Sharma, S. S., Sharma, S., Longhi, P., Colangeli, S., Ciccognani, W., & Limiti, E. (2024, June). Mismatch based implementation of W band LNA using GaAs pHEMTs. In *2024 19th Conference on Ph. D Research in Microelectronics and Electronics (PRIME)* (pp. 1-3). IEEE. https://doi.org/10.1109/PRIME61930.2024.10559742

Tanahashi, N., Kanaya, K., Matsuzuka, T., Katoh, I., Notani, Y., Ishida, T., ... & Matsuda, Y. (2003, June). A W-band ultra low noise amplifier MMIC using GaAs pHEMT. In *IEEE MTT-S International Microwave Symposium Digest, 2003* (Vol. 3, pp. 2225-2228). IEEE. https://doi.org/10.1109/MWSYM.2003.1210607

Thome, F., Leuther, A., Massler, H., Schlechtweg, M., & Ambacher, O. (2017, June). Comparison of a 35-nm and a 50-nm gate-length metamorphic HEMT technology for millimeter-wave low-noise amplifier

MMICs. In *2017 IEEE MTT-S International Microwave Symposium (IMS)* (pp. 752-755). IEEE. https://doi.org/10.1109/MWSYM.2017.8058685

Thome, F., Heinz, F., & Leuther, A. (2020). InGaAs MOSHEMT W-band LNAs on silicon and gallium arsenide substrates. *IEEE Microwave and Wireless Components Letters*, *30*(11), 1089-1092. https://doi.org/10.1109/LMWC.2020.3025674

Thome, F., Brückner, P., Leone, S., & Quay, R. (2021). A wideband E/W-band low-noise amplifier MMIC in a 70-nm gate-length GaN HEMT technology. *IEEE Transactions on Microwave Theory and Techniques*, *70*(2), 1367-1376. https://doi.org/10.1109/TMTT.2021.3134645

Tong, X., Zheng, P., & Zhang, L. (2020). Low-noise amplifiers using 100-nm gate length GaN-on-silicon process in W-band. *IEEE Microwave and Wireless Components Letters*, *30*(10), 957-960. https://doi.org/10.1109/LMWC.2020.3019816

Wang, Y., Lin, F., Sun, H., Wu, H., Xu, C., Fang, Y., ... & Zeng, Z. (2023). W-band GaN T/R single chip with 1-W output power and 6.4-dB noise figure for AESA applications. *IEEE Transactions on Microwave Theory and Techniques*, *72*(2), 1056-1069. https://doi.org/10.1109/TMTT.2023.3304987

Yawei, W., & Weihua, Y. (2013, August). Design and simulation of a W-band broadband Low Noise Amplifier. In *2013 IEEE International conference on microwave technology & computational electromagnetics* (pp. 119-122). IEEE. https://doi.org/10.1109/ICMTCE.2013.6812435

Zhang, J., Lu, Y., & Sun, P. (2018, December). W-band Broadband Low Noise Amplifier Using 0.1−μm GaAs pHEMT Process. In *2018 12th International Symposium on Antennas, Propagation and EM Theory (ISAPE)* (pp. 1-3). IEEE. https://doi.org/10.1109/ISAPE.2018.8634085